Defect Detection in Weld Joints by Infrared Thermography

B. B. Lahiri*, S. Bagavathiappan, T. Saravanan, K.V. Rajkumar, Anish Kumar, John Philip and T. Jayakumar

Nondestructive Evaluation Division

Indira Gandhi Centre for Atomic Research, Kalpakkam-603102

ABSTRACT

The objective of this present paper is to evaluate the effectiveness of infrared thermography (IRT) as a non-contact, fast and reliable non-destructive evaluation procedure for detection and quantification of defects in weld joints. In the present work, a friction stir welded (FSW) joint of two aluminum plates and three 316 LN stainless steel (SS) weld-joints with lack of penetration (LOP), lack of fusion (LOF) and tungsten inclusion (TI) defects respectively, were inspected using IRT and digital radiography (DRG). Using active thermography methods, a sub-surface tunnel defect along the weld line was successfully detected in the FSW joint and its length and width were estimated by suitable pixel calibration. Using lock-in thermography, optimum frequencies were determined for each of the specimens and defect-depths were estimated. Temperature fall of the defect region and defect-free region were monitored as a function of time and it was found that the rate of temperature fall in the former case is slower than that in the latter one. Results from both the techniques, i.e., IRT and DRG were found to be in good agreement with each other in all the cases. Advantage of IRT is that it provides depth information also.

Introduction

Numerous application-specific products are manufactured by joining of two or more similar or dissimilar materials. Welding is one of the most common joining methods used in case of metallic materials [1]. The most common welding methods are gas metal arc welding (GMAW) or Manual Inert Gas (MIG) welding, gas tungsten arc or tungsten inert gas (TIG) welding, plasma arc welding, laser welding, electron beam welding. Generally, process selection is based on the product specification, process capability and cost ([2]. The above mentioned welding processes are routinely used in industries for the fabrication of almost all types of metallic products. Aluminum suffers from weldability problems due to porosity related issues, which occur due to low solubility of hydrogen in solid aluminum compared to the molten state [3]. Friction Stir Welding (FSW) was developed for aluminum-joints in 1991 at The Welding Institute (TWI) [4]. FSW is a solid state joining process where simultaneous presence of frictional heating and forging pressure causes the metal pieces to fuse together to form weld joints and the microstructural characteristics of the original metals remain largely unchanged [5]. FSW has a number of advantages like less porosity, shrinkage and distortion, absence of filler materials and melting resulting in less weld contamination and less process variables to control. This kind of joining is used largely in aerospace, automobile and ship-building industries [2,6]. Although FSW has been extensively used in the joining of aluminum and its alloys, there is a considerable interest in extending the technology to other metals and alloys also, viz., steel [8,9], magnesium alloys [10] and titanium and its alloys [11]. The weld-joints may be the origin of structural weakness in many cases and must be routinely inspected to ensure structural integrity of the products [12]. Most common defects in cases of TIG or MIG welded joints are lack of penetration, lack of fusion and impurity inclusions. FSW is also associated with some unique defects such as surface or sub-surface tunnel defects, kissing bonds and inclusion defects. The defects in weld joints may be discontinuities which may render a part of the weld-joint unable to meet design standards and may cause premature failure of the weld-joints in service or while manufacturing. Hence, there is a wide research interest for inspection and monitoring of weld-joints [13]. Non-destructive evaluation (NDE) of weld-joints is essential to ensure weld-integrity for safe and reliable operation of the fabricated components [14,15]. Farley et al. qualitatively described the importance of NDE in weld inspection by the following relation [15].

Probability of weld failure	= Probability of flaw occurring x Probability of NDE missing defects x Probability of flaw growing

A variety of NDE methods are available for inspection of weld-joints [14,16]. In the present paper Infrared Thermography (IRT) was used to study defects in a FSW aluminum joint and three TIG welded SS joints. The results were verified using DRG technique [17]. IRT is a widely accepted, non-contact and fast NDE technology, where the infrared radiation emitted by a surface is detected using an infrared camera and the information about temperature is obtained using Stefan-Boltzman's law [18]

$$\frac{q}{A} = \varepsilon\sigma \ T^4 \tag{1}$$

Where q is the rate of energy emission in Watts, A is the area of the emitting surface (m^2), T is the absolute temperature (K) and s is Stefan's constant (value = 5.676×10^{-8} W/m^2K^4) and e is the emissivity of the material surface.

In active infrared thermography an external source is required for heating the specimens. Lock-in (LI) thermography is a special type of active thermography, where, the specimen is heated with a modulated heat wave and the data are recorded in stationery domain. In LI thermography, a quantity called thermal migration length (m) is generally used, which provides information about of the depth of defects and is expressed by the following relation.

$$\mu = \sqrt{\frac{2\alpha}{\omega}} \qquad (2)$$

Where α is the thermal diffusivity of the material and $\omega = 2\pi f$, where f is the excitation frequency of the heat waves.

Materials and Experimental Details

Specimen Details

Four rectangular weld-joint (butt-joints) specimens, which include one friction stir welded joint of aluminum alloy and three other TIG welded stainless steel joints, were used in our studies. Details of the specimens are provided in Table I. In all these specimens, defects were artificially created during the welding process itself. A schematic diagram of the specimens is shown in Fig. 1a.

Table 1: Specimen Details

Serial Number	Material	Welding Type	Defect Type	Length (mm) (± 1 mm)	Breadth (mm) (± 1 mm)	Thickness (mm) (± 1 mm)
01	Aluminum alloy (AW-6082)	FSW	Tunnel Defect	250.00	145.00	3.00
02	SS 316 LN	TIG	Lack of Fusion	124.00	98.50	3.20
03	SS 316 LN	TIG	Lack of Penetration	182.50	102.00	3.00
04	SS 316 LN	TIG	Tungsten Inclusion	124.00	97.50	3.25

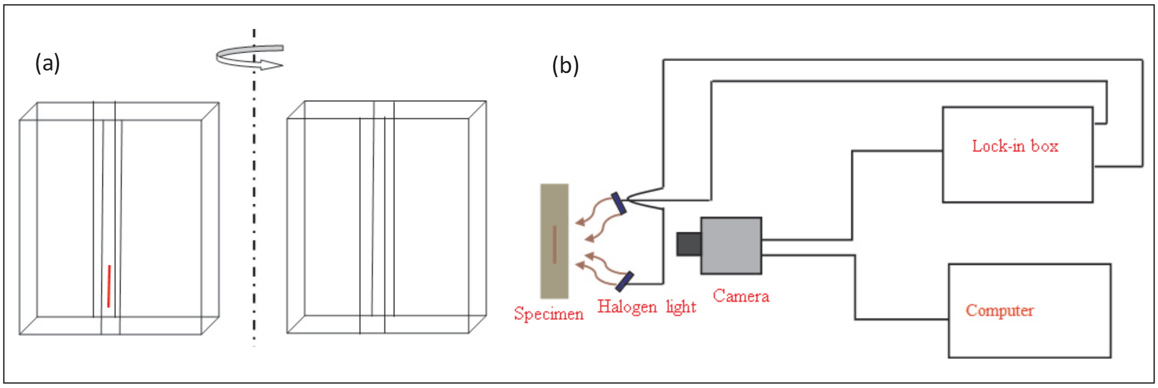

Fig. 1: Schematic diagram of (a) the specimens and (b) experimental set-up for LI IRT

Experimental Details

All the four specimens were inspected by active thermography technique. In case of conventional thermography, the specimens were heated with a 1 kW halogen lamp and the cooling data were monitored in the transient domain. For lock-in thermography, the specimens were heated by a sinusoidally modulated heat wave from two 1 kW halogen lamps kept at 30-35 cm away from the specimen. For the generation of sine waves of a single frequency, a programmable function generator (model: HM 8131-2, Hameg) was used. For the detection of thermal waves FLIR SC5000 infrared camera was used. This camera has indium antimonide (InSb) detector, cooled by Stirling cycle, with an array of 320 × 256 elements. The spectral range is 2.0-5.1 m and temperature sensitivity is better than 25 mK. The camera was kept at a distance of 70-75 cm away from the specimens in such a way that the axis of the camera and that of the specimen were parallel to each other. Both transmission and reflection methods were adopted for conventional thermography, whereas, for lock-in thermography only reflection method was followed. To overcome the emissivity problem a black paint (emissivity   0.98) was applied on the specimen surface. Several excitation frequencies were used to determine the optimum frequency for each of the specimens. The schematic of the experimental set-up for lock-in thermography is shown in Fig. 1b. Radiography was carried out using a 450 kV industrial X-ray unit (Balteau NDT, Belgium) and a flat panel detector (Model: FS 35 Thales Flashscan, with Gd2O2S detector of pixel size 127 m). The radiographic exposure parameters are summarized in Table II.

Table 2: X-Ray Radiography Parameters

Voltage used	125 kV/ 150 kV (for Al & SS respectively)
Exposure	1 mA/ 1mA (for Al & SS respectively)
Source-to-Object Distance (SOD)	950 mm
Object-to-Detector Distance	50mm
No. of Frame integration	25

Result & Discussion

Aluminum weld-joint (FSW)

Figs. 2a & 2b show the normal photograph and IRT image of the FSW aluminum joint respectively. In the thermograph, the defect is clearly visible and a 3D plot of this defect is also shown in the adjoining figure. The thermograph was acquired from the defect free side of the specimen in reflection mode.

Temperature fall as a function of time was monitored for the defect region and defect free region and it was observed that the rate of temperature fall is slower for the defect region, as shown in Fig. 3a. This is due to the difference in thermal properties of the defect and defect-free regions. Length and width of the defect measured from IRT image (59 mm & 0.53 mm respectively) after suitable pixel calibration was found to be in good agreement with the actual dimensions (60 mm &

0.55 mm). From LI IRT experiments it was observed that the optimum frequency for this specimen is 4 Hz (refer to Fig. 3b) and the corresponding thermal migration length was found to be 2.79 mm and this was considered to be the defect-depth. The presence of the defect was also confirmed using DRG. Typical LI IRT and DRG images are shown in Figs. 4a & 4b respectively.

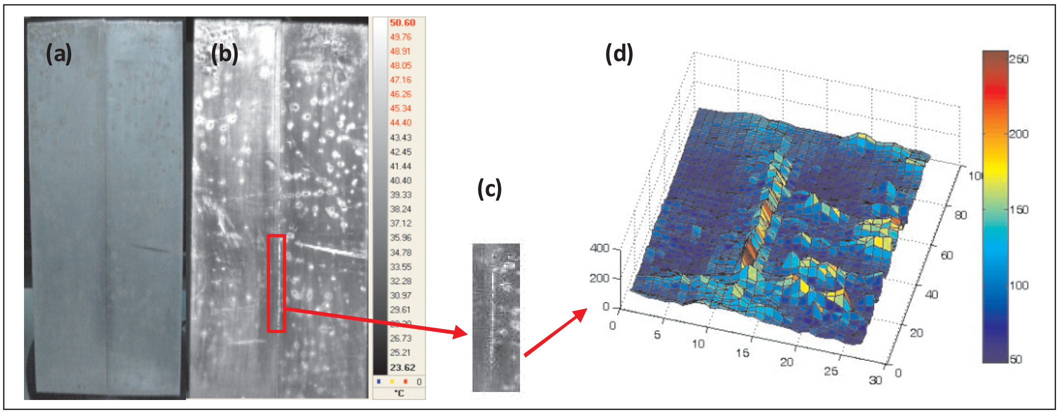

Fig. 2: (a) Normal photograph (b) Thermograph of the FSW weld
(c) Magnified view of the defect-region (d) 3D plot of the cropped defect-region

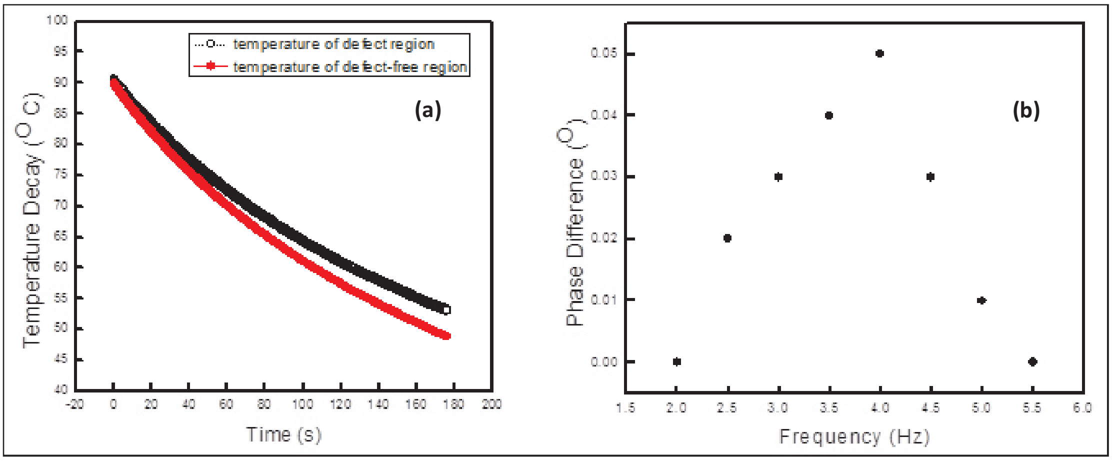

Fig. 3: (a) Temperature fall as a function of time
(b) Phase difference as a function of lock-in excitation frequency in FSW specimen

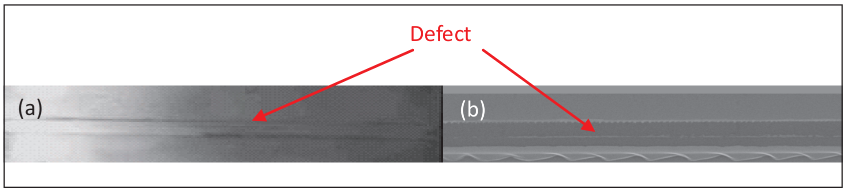

Fig. 4: Typical (a) Lock-in thermography image (b) Digital radiography image of FSW specimen

SS weld-joints (TIG welding)

All the three SS weld-joints were inspected using IRT and defects were identified successfully. Optimum frequencies were determined for each of the weld-joints and the defect-depths were estimated. The defect-depths and the corresponding optimum frequencies are provided in Table III. In Fig. 5a the variation of phase difference with LI excitation frequency for a SS weld joint with LOF defect is shown. The presences of the defects were confirmed by DRG experiments also. Defect locations measured from IRT were found to be in good agreement with that measured from DRG technique, as shown for LOF specimen in Fig. 5b. Typical LI IRT and DRG images of SS weld specimen with TI defect are shown in Figs. 6a & 6b respectively.

Table 3: Defect-depths of SS weld-joints

Name of SS specimen	Excitation Frequency Range (Hz)	Optimum Frequency (Hz)	Defect Depth (mm)
LOF	1.5-0.8	0.1436	3.00
LOP	1.5-0.8	0.1590	2.90
TI	1.5-0.8	0.1266	3.25

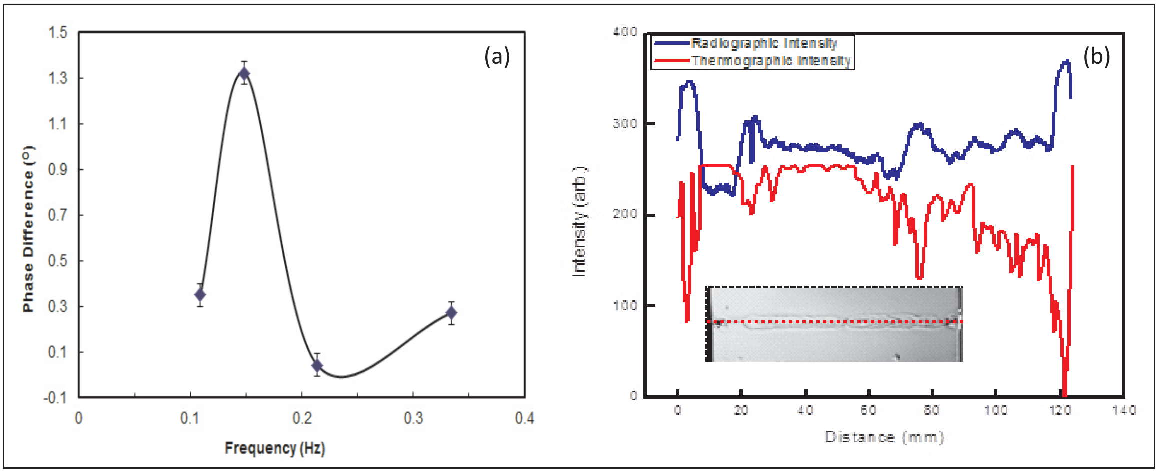

Fig. 5: (a) Phase contrast vs. lock-in excitation frequency (b) Intensity vs. distance along the weld-line for LOF specimen (Inset: Thermogram of SS weld joint with LOF defect)

Conclusion

Defects in a friction stir welded aluminum and three TIG welded SS butt-joints were successfully detected using active infrared thermography and the results were compared with digital radiography technique. The advantage of lock-in infrared thermography over radiography is that the former technique provides information about the defect-depths too. Based on the above studies it was concluded that IRT could be employed as a non-contact and reliable NDE technique for quantitative defect-detection in weld-joints.

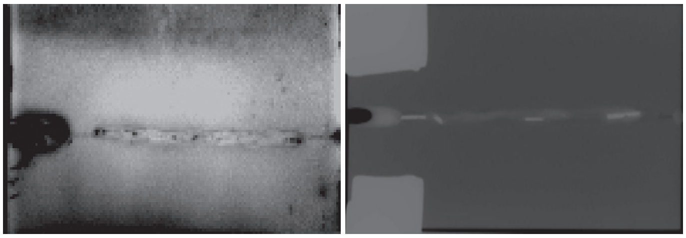

Fig. 6: Typical (a) Lock-in thermography image
(b) Digital radiography image of SS weld joint with tungsten inclusion defects

References

1. C. Davies, The Science and Practice of Welding. Cambridge University Press. 1984
2. N.R. Mandal, Aluminum Welding. Narosa Publishing House. 2005
3. G. Mathers, The welding of aluminum and its alloys: WoodHead Publishing Limited. 2002
4. W.M. Thomas,International Patent Appllication No. PCT/GB92/02203 abd GB Patent Application No, 9125978.8,6 (1991), U.S. Patent No. 5,460,317 (1991).
5. C.G. Rhodes, M.W. Mahoney and W.H. Bingel, Scripta Materialia,36(1997) 69.
6. W.M. Thomas and E.D. Nicholas, Materials & Design, 18,(1997)269.
7. J. Adamowski, C. Gambaro, E. Lertora, M. Ponte and M. Szkodo, Archives of Materials Science and Engineering,28 (2007) 453.
8. W.M. Thomas, P.L. Threadgill and E.D. Nicholas, Science and Technology of Welding and Joining,4(1999) 365
9. L. Cui, H. Fujii, N. Tsuji and K. Nogi, Scripta Materialia,56,(2007) 637.
10. G. Kohn, S. Antonsson and A. Munitz. Friction Stir Welding Magnesium Alloys. in Proceedings of the Symposium on Automotive Alloys, TMS Annual Meeting. 1999. San Diego, California, USA.
11. T.J. Lienert and W.L.S. Jr., EWI Progress Report PR0012,(2000).
12. J.F. Lancaster, Metallurgy of Welding 1999: Abington Publishing.
13. C. Meola, G.M. Carlomagno, A. Squillace and G. Giorleo, Infrared Physics and Technology,46,(2004) 93.
14. B. Raj, C.V. Subramanian and T. Jayakumar, Non-Destructive Testing of Welds: Alpha Science International Limited. 2000
15. J.M. Farley, J.L. Thompson and B.J. Dikstra. Nondestructive Testing to avoid weld failures: a Review. International Conference on Weld Failures. London, England: The Welding Institute. 1998
16. G.R. Edward. (ed). Inspection of Weld Joints. ASM Handbook, Welding Brazing and Soldering. Vol. 6. 1993, ASM International: Materials Park, OH. 1081-1088.
17. R. Halmshaw, Industrial Radiology: Theory and Practice: Springer. 1995
18. X. Maldague, Theory and Practice of Infrared Technology for Nondestructive Testing. Wiley Interscience Publication. 2001